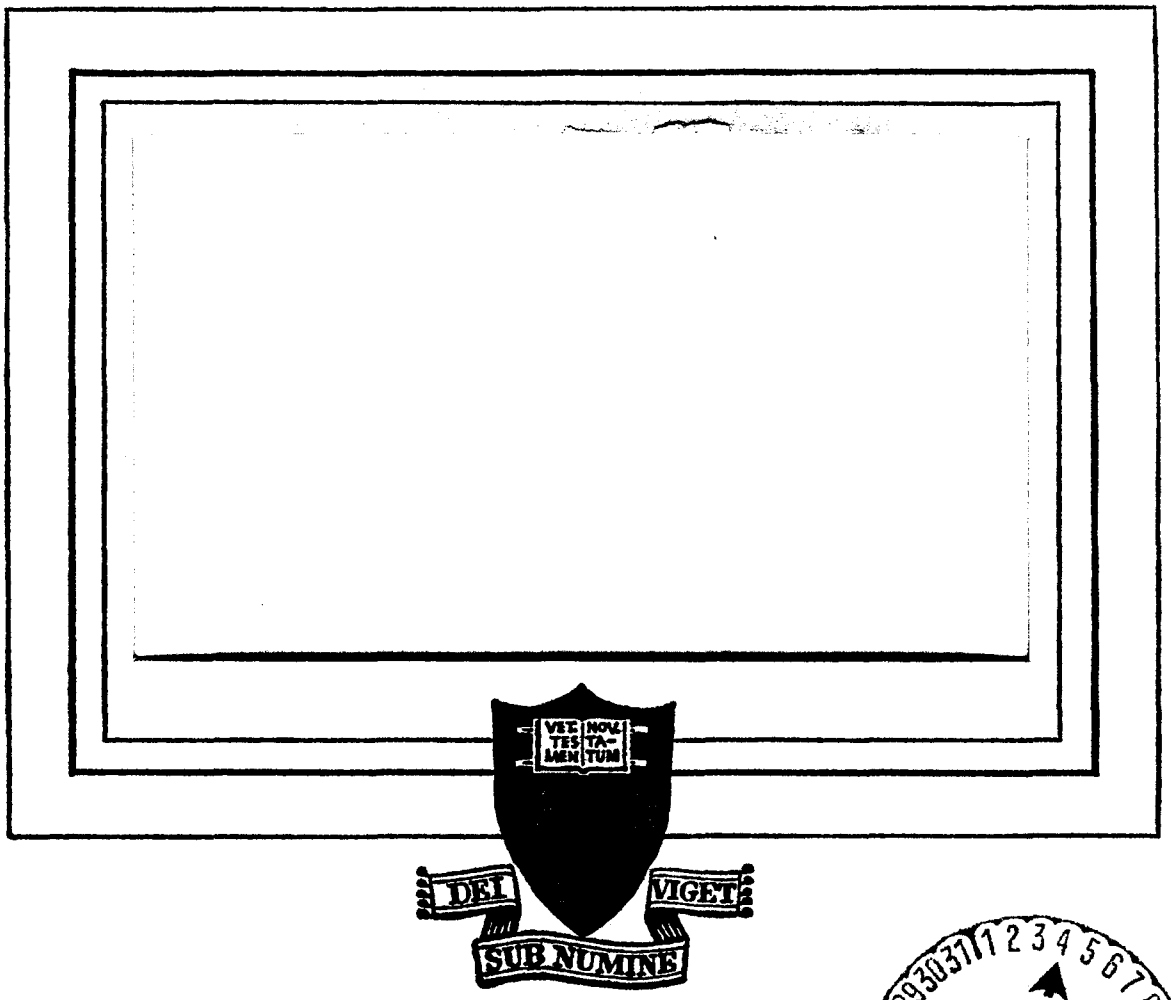

(NASA-CR-127794) DEVELOPMENT OF TELEVISION TUBES FOR THE LARGE SPACE TELESCOPE J.L. Lowrance, et al (Princeton Univ. Observatory) 1971 35 p CSCL 09A

N72-29173

Unclas
G3/09 15662

PRINCETON UNIVERSITY

PRINCETON UNIVERSITY OBSERVATORY
Princeton, New Jersey

DEVELOPMENT OF TELEVISION TUBES FOR THE LARGE SPACE TELESCOPE

BY

JOHN L. LOWRANCE AND PAUL ZUCCHINO

Paper presented at the
International Conference
on
Space Applications of Camera Tubes

November 23 - 25, 1971

Centre National De La Recherche Scientifique
Paris, France

DEVELOPMENT OF TELEVISION TUBES FOR THE LARGE SPACE TELESCOPE

by

JOHN L. LOWRANCE AND PAUL ZUCCHINO

Princeton University Observatory
Princeton, New Jersey, U.S.A.

ABSTRACT

Princeton Observatory has been working for several years under NASA sponsorship to develop television type sensors to use in place of photographic film for space astronomy. This paper discusses the performance of an SEC-vidicon with a 25mm x 25mm active area, MgF_2 window, and bi-alkali photocathode. Results from ground based use on the Coudé spectrograph of the 200-inch Hale telescope are included. The intended use of this tube in an echelle spectrograph sounding rocket payload and on Stratoscope II for direct high resolution imagery is also discussed. The paper also discusses the Large Space Telescope image sensor requirements and the development of a larger television tube for this mission.

INTRODUCTION

Princeton Observatory has been working for several years to develop television type sensors for space astronomy. This work, sponsored by NASA, was initally directed toward an advanced OAO with a 40-inch diffraction limited telescope. Now the emphasis is on the Large Space Telescope (LST), a 3-meter diffraction limited telescope planned for the end of this decade. The primary impact of the LST on the sensor development has been to triple the number of resolution elements for a given angular field of view. The LST application also affords a longer period for the sensor development.

The development program to date has centered around a magnetically focused SEC-vidicon with a usable photocathode and target area of 25 mm x 25 mm. The emphasis has been on achieving low sensor internal background during long exposures, and sensitivity from 1200A° into the visible spectrum. In summary, exposures of 6 hours have been demonstrated on the Coudé spectrograph of the 200-inch Hale telescope, a reliable technique for sealing Magnesium Fluoride windows to the tube has been developed, and high efficiency photocathodes have been made on MgF_2. The television sensor is quantum noise limited over most of its dynamic range and the modulation transfer function (MTF) exceeds 40% at 20 cycles/mm. Environmental tests have demonstrated that the tube can survive the anticipated launch environment. It will be flown as the image sensor in an echelle spectrograph sounding rocket payload next year and a similar TV camera is currently being built by Princeton for Flight 9 of Stratoscope II. This tube, the Westinghouse WX-31718, can be used in the LST with very modest additional development. However, a sensor with higher total resolution would be an advantage in many cases.

A program has been initiated to improve the resolution of the image sensor, both by increasing the MTF in cycles per mm and also by enlarging the image area. The first step is to determine the feasibility of making a higher capacitance SEC target that is 50 mm x 50 mm and able to withstand the rocket launch environment. The current plan is to scale up the existing target and tube. A solid substrate target is also under consideration where the target would be rotated 180° to face the electron gun for readout. The new design is expected to yield at least a factor of 2 improvement in linear resolution and 4 times the number of picture elements per frame. This presumes the new tube will maintain

an MTF of 50% at 20 cycles/mm over the 50 mm x 50 mm format.

We are also exploring the possibility of replacing the SEC target (potassium chloride) with the recently developed electron bombarded silicon diode target which exhibits higher capacitance and target gain at the expense of a substantial temperature dependent target dark current.

The following discussion presents the basis for selecting the SEC-EBS-vidicon type sensor. Optimum matching of the telescope to the sensor is also discussed, as well as other system design considerations.

II. LST IMAGE SENSOR SELECTION CRITERIA

Television type image sensors are expected to be the primary data sensor for the Large Space Telescope. They will be used to record high resolution images in various spectral bands from the far ultraviolet into the near infrared. They will also be used for spectroscopy and may be used in alignment and focus of the optical system.

The selection of the best type of television image sensor for future stellar astronomy space telescopes has been based on the following list of requirements:

Long exposure, with good reciprocity.

Internal tube background sufficiently low so that S/N ratio is quantum noise limited.

High effective quantum efficiency.

Maximum number of picture elements per image, i.e., good MTF in single exposure readout.

Large elemental storage capacity in photoelectrons per picture element.

Sensitive in UV, visible, near IR.

Flat image plane for UV transparent windows.

Sensor Selection

In reviewing the various television type image sensors one notes that the image orthicon and image isocon require a mesh between the photocathode and the target. This mesh only transmits 1/2 to 2/3 of the photoelectrons, reducing the quantum efficiency of the photocathode by a corresponding amount.

In the vidicon there is no mesh prior to signal integration and the effective quantum efficiency of the photoconductor is comparable to the quantum efficiency of the best photocathodes in the visible and substantially higher in the near IR. The EBS or SEC vidicon also have no mesh between photocathode and the integrating target, and it is estimated that at least 95% of the photoelectrons contribute to the stored charge image. Therefore, on the important point of effective quantum efficiency the image isocon and the image orthicon are decidedly handicapped.

Now consider the signal to noise ratio in each type. The electron beam returning from the target of the image orthicon is fed into an electron multiplier. The larger the signal on the target the more beam lands on the target and the less that enters the electron multiplier. The noise in this case is the statistical noise in the image, the statistical or "shot" noise in the electron beam entering the multiplier, and the noise due to the electron multiplier itself. This noise is maximum when the signal is low since that means maximum return beam and therefore maximum beam shot noise. This problem is

overcome by the image isocon where the fraction of the return beam entering the electron multiplier is the electrons which have been laterally deflected or scattered by the charge pattern on the target. Thus the electron beam signal increases as the signal on the storage target increases and the noise is proportional to the square root of the signal. This is a significant improvement over the image the image orthicon. A detailed analysis of the isocon S/N is beyond the scope of this paper, but in summary the S/N over the entire dynamic range is still considerably below the statistical S/N of the image stored on the target.[1]

In the case of the vidicon, the signal is due to the electrons landing on the target and this signal is normally fed to a preamplifier rather than electron multiplier. The noise level of the best preamplifiers is 300 to 400 electrons rms per half cycle of bandwidth. This means that the noise due to the readout process is comparable to statistical noise in 100,000 photoelectrons per picture element. Return beam versions of the vidicon suffer from the same limitations as the image orthicon and isocon.

The EBS or SEC vidicon employing the same preamplifier as the vidicon have the advantage of pre-storage target gain. Thus the preamplifier noise is reduced relative to the statistical noise in the photoelectron image by the target gain. With an SEC gain of 70 this means the readout threshold is 400/70 or 6 photoelectrons rms, and the gain of 2000 with the EBS tubes silicon target makes the preamplifier noise negligible.

So, on the question of achieving a quantum noise limited S/N ratio, tubes with high prestorage gain have a clear advantage.

Another important point is resolution in cycles per unit length. The orthicon is at a disadvantage due to the fact that the signal charge is stored between the target and the target mesh. When sensed by the electron beam the charge image appears somewhat defocused or diffused due to the finite spacing between target and mesh of 12 to 25 microns. With the SEC or EBS vidicon the target thickness can be considerably thinner with correspondingly higher resolution.[1] The vidicon has the highest intrinsic resolution due to the very thin photoconductive target which can be made less than a micron thick.

The remaining very important characteristic is long exposure capability. The orthicon can be made with a high resistivity glass target capable of integrating for many hours. The EBS silicon target is limited by the dark current of the silicon diodes. At room temperature the integration periods is in the order of seconds. When cooled to -40°C the integration period is several minutes. The photoconductive target is also limited by dark current. Cooling reduces the dark current and allows longer integration periods.

The following tabulation summarizes the reasons for selecting the SEC or EBS vidicon and the primary reasons for rejecting the other types for this particular application.

Image Isocon and Image Orthicon are rejected for the following reasons:

a. the target mesh collects a large fraction of the photoelectrons, lowering the net quantum efficiency of the photocathode;

b. the target-mesh arrangement creates a charge image that seriously degrades the MTF in single exposure readout.

Vidicon and Return Beam Vidicon are rejected for the following reasons:

a. the absence of prestorage gain in the target makes it impossible to achieve a quantum noise limited signal due to preamplifier noise or beam shot noise with return beam readout;

b. the dark current of the photoconductor requires cryogenic cooling for long integration.

Reasons for choice of SEC-vidicon, or EBS-vidicon type tube:

a. absence of target mesh, therefore no photoelectron attenuation;

b. target gain is sufficient to make preamp noise negligible when referred to photocathode;

c. target capacitance is large enough to allow collection of several thousand photoelectrons per picture element;

d. modulation transfer function in single exposure readout is acceptable;

e. in the case of the SEC-vidicon the integration time is hours, and with the silicon target EBS-vidicon several minutes long integration is possible with modest cooling.

III. SYSTEM DESIGN CONSIDERATIONS

In developing the particular sensor for this important mission one must consider the actual mission in some detail. The following discussion addresses several important image sensor system considerations.

Multiple Short vs Long Exposures

There appears to be a tradeoff between sensors that can integrate for about several minutes and the SEC-vidicon that can integrate for many hours. This is particularly important since most exposures with the LST will be interrupted for 30 to 60 minutes each 90 minute orbit period due to the earth occulation or because of scattered light. The most interesting tradeoff is between the SEC-vidicon and the EBS-vidicon, similar tubes with different types of targets.

	SEC	EBS
Target Gain, G,	50 to 100	1000 to 2000
Target Capacitance,* C,	2×10^{-12} f/mm^2	40×10^{-12} f/mm^2
Target Capacitance referred to the photocathode, C/G,	2×10^{-14} f/mm^2	2×10^{-14} f/mm^2

*Target capacitance can be increased to some extent for both the SEC and EBS. Values used represent currently available values.

The capacitance of the target in photoelectrons per unit area is approximately the same, 400 per pixel at 20 cycles/mm and 4 volt target swing. The readout noise in each case is the preamplifier noise. The preamplifier noise referred to the photocathode is divided by the target gain. For a preamp noise of 500 electrons per half cycle of video bandwidth:

	SEC	EBS
Readout Noise in Photoelectrons	$\frac{500}{70} = 7$	$\frac{500}{2000} = 0.25$

One sees that the readout noise is negligible in the case of the EBS tube due to the high target gain.

Therefore the EBS tube allows readout at a photoelectron threshold a factor of 30 lower than the SEC. This means that the same readout noise level would accrue after $(30)^2$ readouts of the EBS tube since the noise adds quadratically. Presuming the EBS tubes integration time to be 2 minutes the equivalent total exposure based on readout noise is then 30 hours.

Now consider the silicon target dark current as a noise source. At -40°C the diode dark current of the silicon target is 10-12 ampere per sq. mm. At a resolution of 20 cycles/mm the number of dark current electrons per picture element per second is:

$$\frac{10^{-12} \times \left(\frac{1}{40}\right)^2}{1.6 \times 10^{-19}} = 4000 \text{ electrons per second}$$

Referred to the photocathode that is 2 photoelectrons per second. The "full target" capacity in photoelectrons per pixel referred to the photo cathode is:

$$2 \times 10^{-14} \text{ f/mm} \left(\frac{1}{40}\right)^2 \quad \frac{1}{1.6 \times 10^{-19} q} \quad 5 \text{ volts} = 400 \text{ photo electrons/ pixel}$$

C/G	ratio of pixel area at 20 Cycles/mm to 1 mm^2	coulomb/ electron	practical target swing

So a target dark current of 10^{-12} amp/mm^2 fills the target in 200 seconds.

The shot noise in the dark current image on the target is:

$$\sqrt{(4000 \text{ e/s}) \ 200 \text{ sec}} = 900 \text{ rms electrons} = \tfrac{1}{2} \text{ photoelectron}$$

The "target filling" action of the dark current is a much more important limitation than the shot noise associated with the target dark current. A greater noise background may be the fixed pattern background due to variation in the dark current characteristics of each of the many diodes on the target. This can be calibrated out in computer processing the data.

One must consider on board storage of the short exposures. This can be accomplished via magnetic tape recorder or solid state components; not an overriding factor but as noted later each frame may contain approximately 10^8 bits of data.

The SEC-vidicon can store the image almost indefinitely until readout to the ground station if desired. This could be a real advantage for some smaller satellite applications and does allow data to be obtained in the event of tape recorder failure.

Discrete Photon Counting Image Systems

There is considerable interest in television systems that can be used to detect a single photoelectron and its location in a two-dimensional image. In such a system the image must be integrated in an external digital memory. The primary advantage of this system is unlimited integration time. It may also afford a lower system noise threshold for very weak exposures of only a few photoelectrons per picture element. A third advantage may be in photometry of wide dynamic range images.

In considering such a system for space, the large memory is the first obstacle. To duplicate the capability of the current 25 mm x 25 mm target SEC vidicon, one requires a memory of 10^8 bits that can be scanned in a fraction of a second. While this is within the state of the art, the power and weight are certainly excessive in comparison to the integrating television system. Rapid strides are being made in the state of the art of memories and the memory system characteristics may be much more reasonable in a few years.

In summary, the development of the two dimensional photon counting systems is much less advanced than the integrating TV system. Therefore it is not possible at this time to compare the relative effective quantum efficiencies and observational advantages of the two approaches. Both systems will probably find application in space astronomy missions like the Large Space Telescope.

f-Number Concept for TV Sensors

For extended objects the common equation for the flux density in the image plane of an optical system is given by:

$$E^* = \frac{E}{4f^2} \qquad (1)$$

where

E = scene luminance

E^* = image illuminance

$f = \frac{\text{Diameter of Entrance Aperture}}{\text{Focal Length}} = \frac{D}{F}$

For photographic film this expresses the "speed" of the system very well. However, with certain television type sensors it is more useful to express the image illuminance in terms of energy per picture element and energy per solid angle.

Let h = height of the picture element in the image plane

h^2 = the area of a picture element and

$E^* h^2$ = energy per picture element

Rewriting equation (1)

$$E^* h^2 = \frac{E D^2 h^2}{4 F^2}$$

The solid angle subtended by the picture element is $\left(\frac{h}{F}\right)^2$, and the image illuminance in energy/solid angle = $\frac{E D^2}{4}$

Therefore, for a given angular resolution the flux per picture element is only a function of the entrance aperture, D^2.

The ratio $\frac{h}{F}$ is adjusted for the desired angular resolution. The value F should be as large as practical to maximize the MTF (modulation transfer function) of the image sensor and in some cases the optics. The total angular field of view is:

$\Theta = \frac{h}{F}$ x Number of picture elements across the image sensor or for a fixed image sensor size "L"

$\frac{L}{h}$ = Number of elements, and $\Theta = \frac{L}{F}$

There is then a straightforward system tradeoff between the field of view and MTF for a given image sensor size.

Choice of f-Number for LST

The limiting spatial frequency of the 120-inch telescope is expected to be $\frac{2a}{\lambda}$ cycles/radian or $0.16 \times 10^{-6} \frac{\text{radian}}{\text{cycle}}$ at 5000A° over a field of view of about 4 arc minutes. At a cassegrain focal ratio of f/15 the 4 arc minute field is 52.5 mm wide and the limiting spatial frequency corresponds to 138 cycles per mm. The total number of picture elements is 14,500 x 14,500 where each picture element is taken to be one half cycle of spatial frequency.

One sees that the information gathering capability of the LST is indeed remarkable. At f/15 there is no image sensor that can match this resolution and field without seriously degrading the data. The focal length must be increased at the expense of the field of view. If one expects to obtain useful data the

the sensor must have adequate response at the telescope's limiting spatial frequency. The problem is particularly acutre if the scene is low contrast to begin with as in the case of planets, very faint stars, and weak spectral lines. If one specifies that the limiting resolution can be degraded by no more than 50%, then the focal length must be adjusted to match the capability of the sensor. For example, let the spatial frequency be 20 cycles/mm: focal length,

$$F = \frac{1/20 \times 10^{-3}}{0.16 \times 10^{-6}} = 312 \text{ meters}$$

and the f-number is f/104.

In cases where the problem is detection, as in the case of stars below the sky background, it is advantageous to contain all the collected signal from the star within one half cycle of the video bandwidth, i.e. one picture element. At the same time, the physical size of the picture element should be consistent with good spatial frequency response of the sensor. To maximize detectivity, all of this energy should be collected on one picture element. This can be done by reducing the f-number by 4.88 or by reducing the video bandwidth and increasing the width of the scan lines by the same factor such that a picture element is physically larger on the target of the tube.[2] In the latter case the spatial frequency of interest is now 20/4.88 cycles/mm and the MTF is near 1.0, an added advantage in detectivity. On the other hand the background noise in the image sensor (Fig. 2) is higher at lower spatial frequencies. The best system design in this case must consider the actual levels of sensor background relative to the image low frequency signal, the actual sensors MTF and the ease of implementing the two approaches.

Dynamic Range and Contrast Considerations[2]

The modulation transfer function of a diffraction-limited telescope is shown in Fig. 1. Note that the wide variation in attenuation over the spatial frequency range necessitates a minimum dynamic range for the image sensor. At 0.8 l.s.f. (limiting spatial frequency) the response is 10% of the low frequency response. The scene contrast at high spatial frequencies will in most cases be lower than at low spatial frequencies, increasing the ratio of high frequency to low frequency signal in the image even further. Table I shows the electrical image dynamic range versus the scene contrast at 0.8 l.s.f., and their relation to the total number of photoelectrons per picture element. It is sobering to note that, with a background (low frequency) quantum signal-to-noise ratio of 100, a 33% contrast high-frequency signal is only three times the r.m.s. noise of the background as imaged by the diffraction-limited telescope. Mariner IV pictures of Mars show a typical surface contrast range of 15 to 30%.

There is interest in rectification of the recorded images to remove the spatial frequency attenuation of the telescope and image sensor using optical or digital-computer data processing techniques. The degree to which the attenuated high frequency components can be amplified or "peaked" is directly related to the signal-to-noise ratio at these high spatial frequencies.

From this analysis it can be concluded that in order to take full advantage of the limiting resolution of the telescope, the image sensor system must have the capability of integrating a large number of photoelectrons per picture element. The limited capacity of the storage targets in available sensors requires that in some cases a portion of the integration be carried out ex post facto in auxiliary equipment such as a digital-computer.

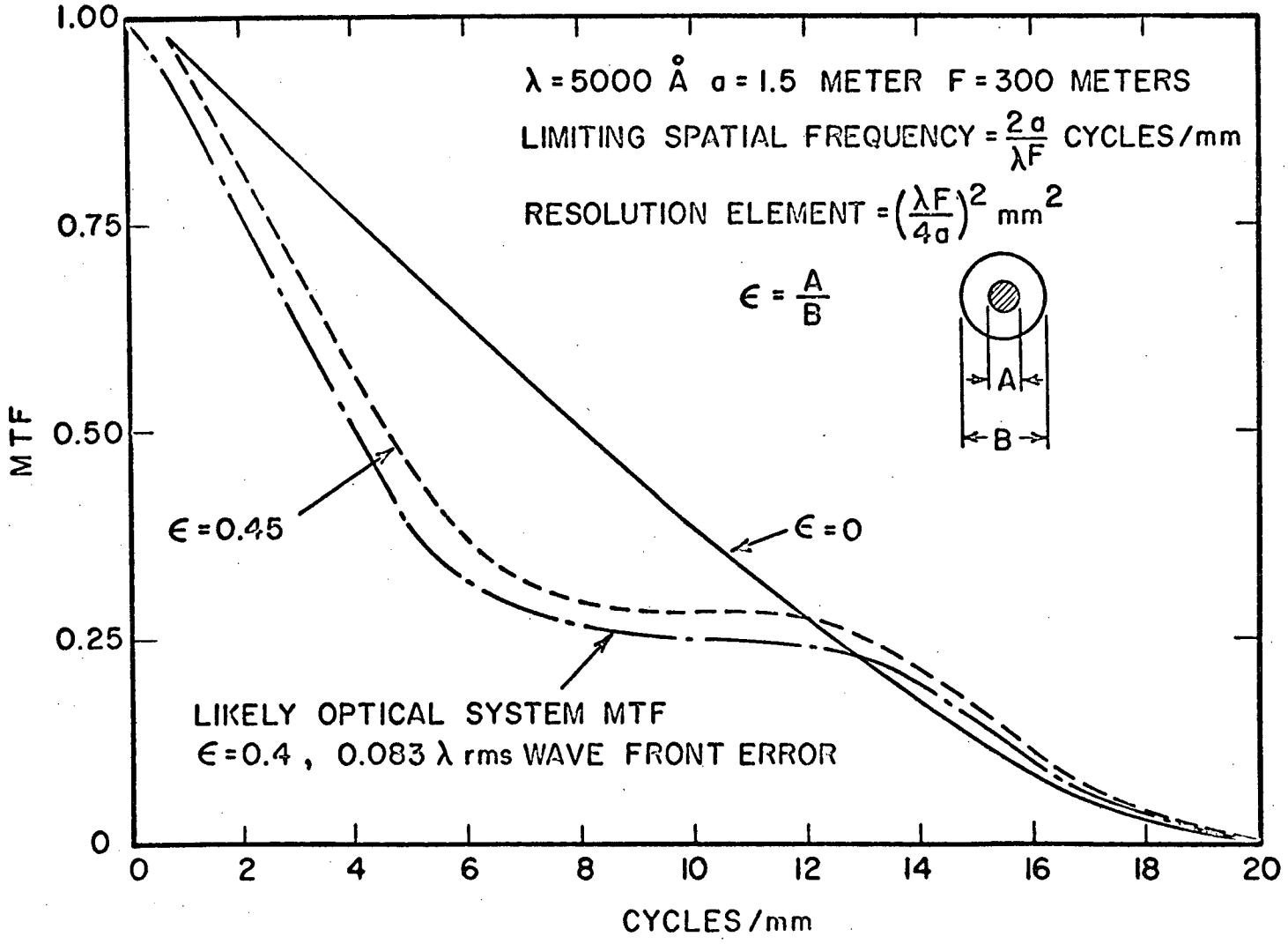

Figure 1 - Modulation Transfer Function of 3 Meter Diffraction Limited Telescope.

TABLE I

Scene Contrast versus Sensor Integrating Capacity

Low Frequency signal (photoelectrons/ image element)	Quantum noise	Detectable Threshold 3 σ high frequency signal	Optical signal necessary with optical attenuation of 10 : 1 at 0.8 l.s.f.	High frequency to background scene contrast	Electrical image contrast, Sensor MTF=50%
10^3	33	100	1000	1	1/20
10^4	100	300	3000	1/3	1/66
9×10^4	300	900	9000	1/10	1/200

σ = mean square deviation; coefficient of certainty k = 3

In recording spectra there is the important advantage of being able to increase the effective capacity of the sensor in terms of photoelectrons per Ångstrom by trailing the spectra normal to the dispersion as is often done in photographic recording of spectra. The earlier discussion of dynamic range and contrast is equally relevant to spectra. In measuring absorption or emission against a continuum, there is the advantage of knowning roughly where in the dynamic range the high frequency detail of interest is located, i.e., on top of a continuum that may vary by a factor of two or three over the spectral range being recorded. In order to measure an absorption of 1% such that it is three times the mean square deviation in the continuum, i.e., 3σ confidence, the quantum signal-to-noise ratio of the continuum must be at least 300. This in turn requires that 9×10^4 photoelectrons per spectral resolution element be collected.

Noise As A Function Of Spatial Frequency

The signal to noise ratio is often expressed as the ratio of the low frequency or DC signal to the noise at full system bandwidth, i.e., full spatial frequency response. It is more informative to express the S/N ratio as a function of spatial frequency.

The sensitivity of the television sensor is expressed as signal electrons from the target per photoelectron from the photocathode. In the readout of the signal electrons there is a noise threshold due to the preamplifier which is expressed in electrons per half cycle of video bandwidth. This noise threshold is due to the preamplifier alone and is independent of the actual dimension on the target that is scanned by the beam during the time period of a video half cycle.

The other noise sources in the signal are:

a. quantum noise in the signal;
b. quantum noise in the background;
c. noise in the read beam switching;
d. variations in target gain.

The background noise is made of the DC background in the signal itself, plus the background due to dark current emission from the photocathode and other parts of the image section. There is a somewhat different background due to the need to shift the target voltage before readout by the electron beam. This shift insures that the electron beam lands in the lightly exposed area of the image.

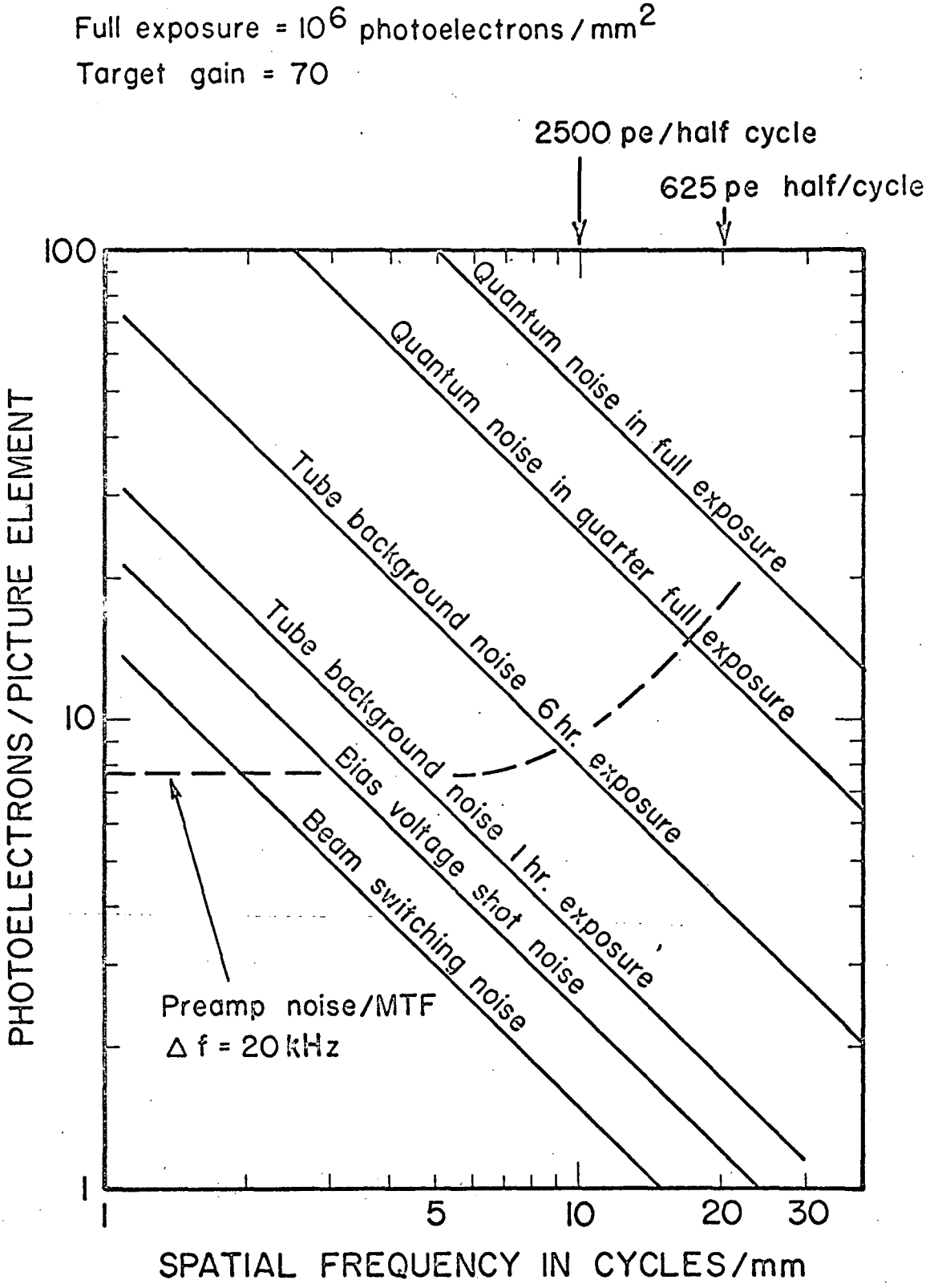

Figure 2 - SEC-Vidicon Noise vs. Spatial Frequency.

RC

Now let's examine the various noise components as a function of spatial frequency on the target.

The quantum noise in the optical background is the square root of the number of photoelectrons in the background of the optical image.

The ratio of background to signal is the image contrast and is independent of the optical magnification, i.e., spatial frequency at the sensor.

The total thermal and field emission induced dark current background is proportional to the area of the photocathode. The internal background expressed in photoelectrons per resolution element is proportional to the actual area of the picture element. Therefore, for a given tube this background decreases as the square of the sensor spatial frequency, and the noise due to this background is inversely proportional to the spatial frequency.

The readout target voltage shift can be expressed in photoelectrons.

The SEC vidicon target capacity is about 2×10^{-12} farad/mm^2

Let the bias voltage be 0.5 volt

$$Q = CV = 10^{-12} \text{ coulomb/mm}^2 \text{ or } 6 \times 10^6 \text{ electrons/mm}^2$$

at 10 cycles/mm this becomes

$$\left(\frac{1}{20}\right)^2 \quad 6 \times 10^6 = 15 \times 10^3 \text{ electrons/half cycle}$$

the noise would be $\sqrt{1.5 \times 10^4} = 122$ electrons/half cycle rms

and at a target gain of 70 this is equal to 1.8 photoelectrons/half cycle rms.

This target bias voltage noise is also inversely proportional to the sensor spatial frequency, but is relatively small in any case.

The read beams switching noise is a function of the electron beam cathode temperature and elemental target capacitance.[3]

$$\overline{q_n}^2 = 2 \text{ k TC}_s$$

at 10 cycles/mm this becomes

$$= (2)\ (1.38 \times 10^{-23} \text{ joule/°K})\ (1100 \text{ °K})\ (0.5 \times 10^{-14}) = 1.518 \times 10^{-34}$$

$$q_n = 1.22 \times 10^{-17} \text{ coulomb} = 77 \text{ electrons} = \frac{77}{70} \text{ or} \approx 1 \ \frac{\text{Photoelectron}}{\text{half cycle}} \text{ rms}$$

So one sees that the dominant readout noise is the preamplifier noise or the noise in the optical input signal; Both of which are independent of the actual spatial frequency at the photocathode or storage target of the sensor. This is shown graphically in Figure 2.

Only in the case of several hour exposures does the system noise become spatial frequency dependent because of the internal background. Even this is not relevant in the region of interest, i.e., 20 cycles/mm where the tubes MTF approaches 50%. In many applications the dominant noise will be the quantum noise in the optical image.

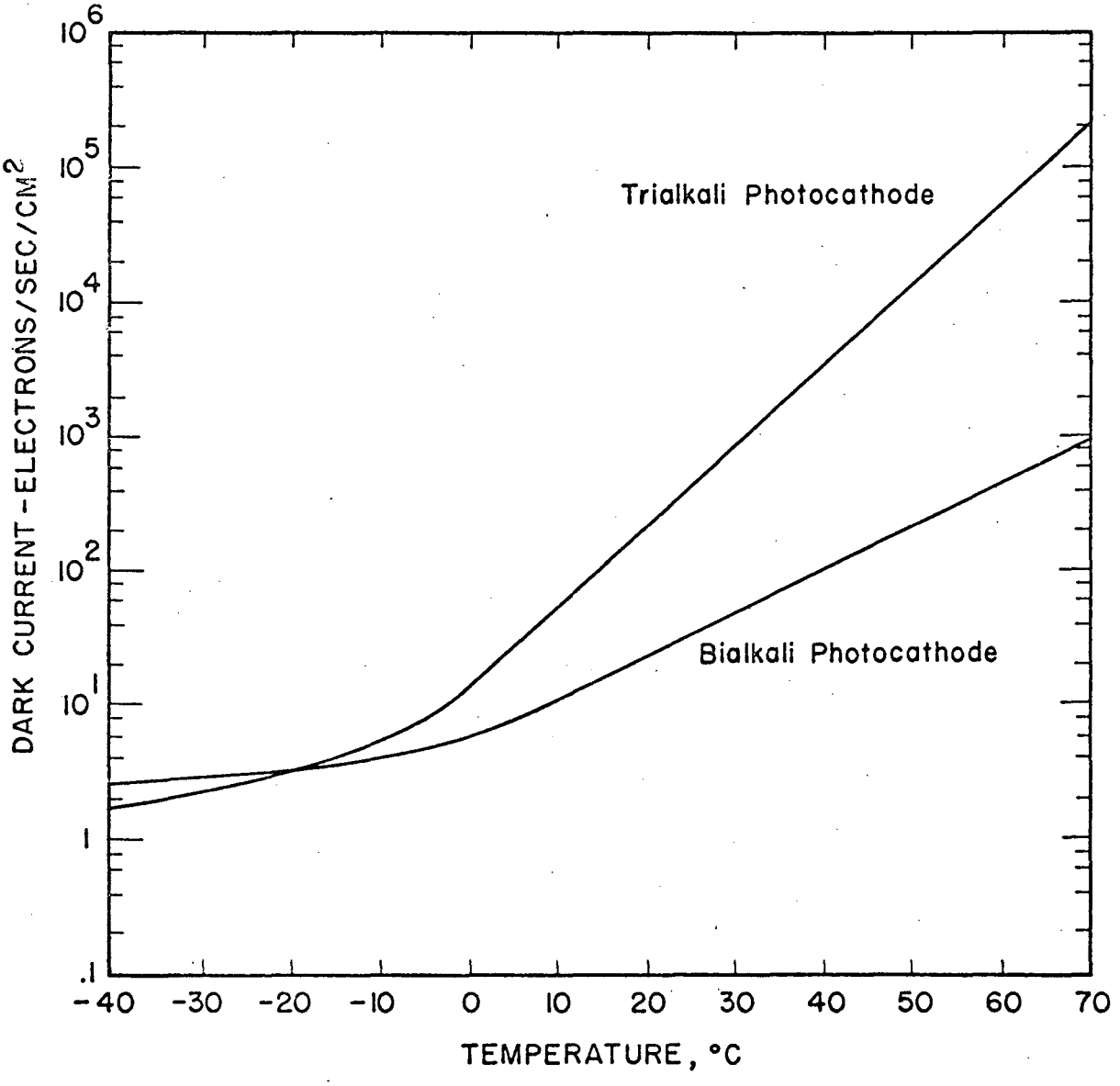

Figure 3 - Photocathode Dark Current vs. Temperature.

The cosmic ray background is only 0.5 particles/cm^2 /sec/ster above 40 mev. The high energy proton density above 40 mev is a strong function of altitude and longitude. At 300 nm altitude the proton density exceeds the cosmic ray background only in the south Atlantic anomaly. Presuming a total dose of 1500 protons/cm^2 /sec due to a pass through the south Atlantic anomaly the Cerénkov radiation should not exceed 3×10^6 photoelectrons per cm^2. At 20 cycle/mm resolution this is approximately 20 photoelectrons per picture element per orbit. This is tolerable and could be decreased for very long exposures by shutting off the system during the transit through the high flux region.

MTF Effect on Signal and Background Noise

The MTF of the image sensor and optical system represents a filter which attenuates the higher spatial frequencies in the image.

Consider the effect of this filter on the quantum noise in the signal and the background. The quantum noise is the statistical variation in the number of quanta measured or counted. This statistical variation has no spatial component except that the number measured is proportional to the size of the picture element. Therefore the MTF of the image section of the sensor does not attenuate the quantum noise, only the spatial information in the signal. The MTF of the target and electron beam readout of the image sensor does have equal effect on the signal readout process and the quantum noise due to the background.

Integrating TV S/N

MTF_1 = optics MTF

MTF_2 = image section MTF

MTF_3 = readout section MTF

N_s = high frequency signal

N_B = low frequency background signal

N_r = rms readout noise expressed in photoelectrons

$$\text{High Frequency S/N} = \frac{N_s\,(MTF_1)\,(MTF_2)\,(MTF_3)}{\sqrt{(N_B + N_s)\,(MTF_3) + (N_r)^2}}$$

Image System Data Rates

The average data rate of the imaging system in most cases will be limited by the rate at which photons are collected by the telescope. Table II gives the limiting data rate for various likely objects presuming a 3-meter telescope and a 1000 A° wide spectrum. One will note that except for the nearer planets, the data rate is quite modest. And in the case of the planets, the spectral band will probably be a few angstroms rather than 1000 A°, so the data rate will also be relatively low.

The optimum rate of reading the data out of the image sensor is dependent on the signal readout technique. If the signal is taken at the target signal plate, the optimum rate is a function of the capacitance to ground of the electrical network at the preamplifier input. With the current 25 mm x 25 mm target SEC-vidicon the optimum bandwidth is approximately 20 kHz. With return beam readout the readout noise is primarily the beam shot noise which is essentially independent of the video bandwidth.

In most cases the analog data will be digitized before transmission and

Planet	Magnitude (visual)	Radius (sec of arc)	Diameter in resolution elements	Diameter at f/200 (mm)	Photoelectrons/ sec per element (0.02" x 0.02"), = 1000 Å, = 150 cm, 10% efficiency	Exposure time for 10^4 photoelectrons per element* (sec)	No. of resolution elements in image	Maximum Digital Data Rate(bits/sec) Sampling Factor 1.4, Horizontal & Vertical 9 bits per sample**
Mercury	-1.8	2.51	250	15	755,000	0.013	49,000	14,700
Venus	-3.5	4.84	482	29	970,000	0.01	183,000	55,000
Mars	-1.98	8.94	895	53.5	70,500	0.14	625,000	187,500
Jupiter	-2.50	23.43	2350	141	17,650	0.57	4,320,000	1,300,000
Saturn	+0.7	9.76	975	58.5	4,940	2	750,000	225,000
Uranus	+5.51	1.8	180	10.8	1,700	5.9	25,400	7,600
Neptune	+7.85	1.06	105	6.36	562	17.8	8,800	2,640
Pluto	+14.87	0.11	11	0.66	83.5	121	94	14
NGC 6826, planetary nebula	+9.3	13	1300	78	0.94	10^4	1,330,000	2,400
Crab nebula	+8.6	150	15000	900	0.014	7×10^5	1.77×10^8	4,560
Star	+18	–	4.88	0.244	67	150	18.7	2.2

Table II

Typical Objects for High Resolution

Imaging with 3-meter Diffraction Limited Telescope

* Adequate for 33% scene contrast at 0.8 limiting spatial frequency.

** Limited to maximum rate of 1 picture per minute.

probably before on-board storage. The number of bits per picture sample must be large enough to make the "quantizing" noise small compared to the noise in the analog data.

The peak to peak signal to rms noise ratio due to this quantizing noise is:[4]

$$S/N = \sqrt{12}\ M$$

where M is the number of levels.

No. of bits	M	S/N
4	16	55.2
5	32	111
6	64	222
7	128	444
8	256	888

One must also consider the digital sampling rate relative to the limiting spatial frequency and video bandwidth.

The Nyquist criteria states that the minimum sampling rate must be equal to once per half cycle of the highest frequency of interest.[5] On further examination one notes that this minimum sampling rate results in low pass filtering $\left(\frac{\sin x}{x}\right)$ of the signal with 63% response at the frequency equal to $\frac{1}{2}$ the sampling rate. Therefore in most cases the sampling rate should be greater than the Nyquist minimum. If the rate is 3 times the maximum frequency, then the filter response is 0.83 and for 4 samples per cycle is 0.9.

If one takes the sampling to be 4 times per cycle of limiting spatial frequency of a diffraction limited 3-meter telescope, which is 30 cycles/$\widehat{sec}$., and if 8 bits are used to encode the information per sample, the information density per square second of arc is 115,200 bits/$\widehat{sec}^2$. If the high resolution field is imaged at f/100, a 50 mm x 50 mm format subtends a 34.3 x 34.3 $\widehat{sec}$ field. The information content per frame is $(34.3)^2 \times 115{,}200 = 1.35 \times 10^8$ bits/$_{frame}$.

Thermal Design and Permanent Magnet Focus

The photocathode dark current and other background currents within the image section are strongly influenced by temperature. Figure 3 shows the photocathode dark current vs. temperature for bi-alkali and tri-alkali photocathodes.[6] Based on overall measurements of the tube background, one concludes that the total background obeys the same trend. There is then a clear argument for keeping the image section of the television sensor cool, preferably below -20°C. The silicon target tube, EBS-vidicon, requires even lower temperatures to limit the target dark current.

The preferred cooling scheme is to put the sensor in a cold environment and minimize the heat dissipated by the television camera. This has led to the development of a permanent magnet assembly to provide the focus field of the television tube. The alternative of electrostatic focus is unacceptable because of lower MTF and geometric distortion. The 80 gauss focus field, when electro-magnetically generated, requires about 10 watts in a practical design for the 25 mm target tube. A 50 x 50 mm target tube would require approximately 60 watts.

The current permanent magnet focus assembly is shown schematicly in Figure 4. It provides an 80 gauss field generated by the two axially magnetized permanent magnets. The field is flattened by tapering the wall thickness of the inner

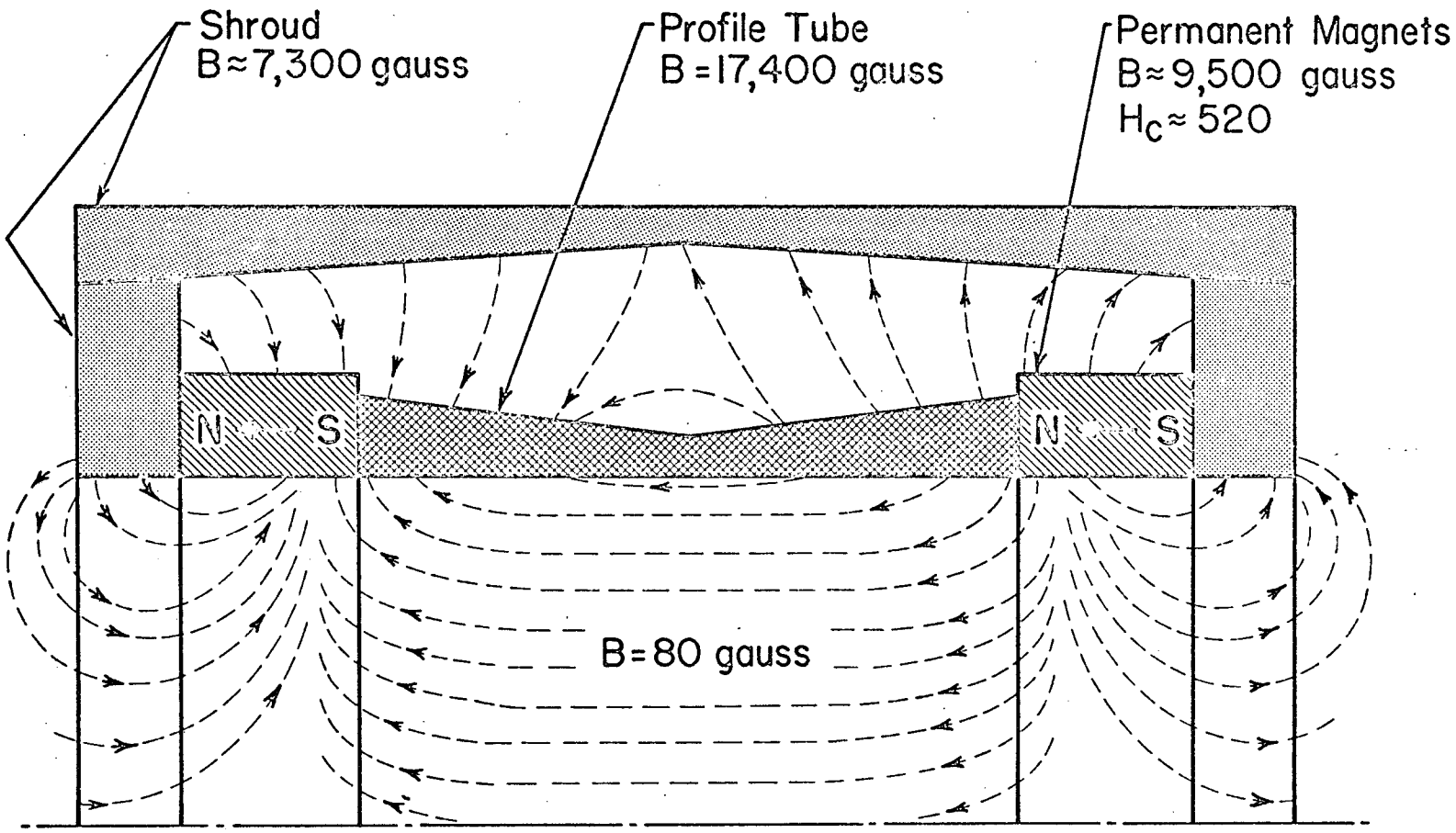

Thickness of profile tube is tapered such that the flux density (B) in the iron is constant having a value of 17,400 gauss. The magnetizing force (H) required to sustain this field is 80, thus producing an axial field of 80 gauss within the interior of the cylinder.

Figure 4 - Permanent Magnet Focus Assembly.

cylinder connecting the two magnets. The return path through the outer shell minimizes the stray field. This stray field is an important consideration in space applications because of the moment generated from interaction with the earth's field and the resultant effect on the pointing stability of the satellite. This will be minimized to some extent by having pairs of television cameras with opposite polarity fields mounted close together. Two cameras are recommended for reliability as well. Any residual magnetic moment can be bucked out with an auxillary coil not necessarily located in the instrument compartment.

Photometric Transfer Function

The SEC target consists of a "fluffy" dielectric layer of KCl supported by a substrate made of Aluminum Oxide coated with Aluminum to form the signal electrode. The aluminum layer on one side of the target and the scanning electron beam on the other side complete the electrical circuit with the target being capacitive. The exposure process with photoelectrons penetrating the dielectric layer causes selective discharge of the charge across the capacitor. As the voltage across the capacitor drops the discharge per photoelectron decreases. This is somewhat analogous to the exponential response of the RC electrical network but differs in the details of the charge flow or leakage. The net effect is a decrease in the target gain expressed in Δ Q/photoelectron. This characteristic is shown in Figure 5. It appears to be uniform in shape throughout the target. The gain of the target does vary in different areas and this variation must be corrected for in the data reduction.

In the case of the silicon diode target, the target gain is constant as a function of exposure and proportional to the accelerating potential between photocathode and the target.

Figure 5 shows the photometric transfer function for the 25 mm x 25 mm SEC-vidicon. The maximum exposure is somewhat arbitrary, but is normally around 1800 photoelectrons per picture element. The readout noise is about 8 photoelectrons rms per picture element. One notes that the signal to noise ratio closely approaches the quantum noise limited S/N over most of the dynamic range.

Spectral Sensitivity

The emphasis in this program has been on developing a sensor that would be sensitive from the visible as far into the ultraviolet as possible. Some ultraviolet sensors use a wavelength conversion layer on the exterior face of the sensor window. These luminescent phosphors emit photons in the visible spectrum and have a quantum efficiency approaching 1. Unfortunately the emitted photons have a Lambertian spatial distribution with the result that half the radiation is emitted in the backward direction away from the faceplate. Optimistic estimates of the net quantum efficiency are in the order of 4%.

Lithium Fluoride will transmit down to 1050A°. Unfortunately its transmission is seriously degraded by bombardment by energetic particles. Magnesium Fluoride will transmit down to 1150A°, and is much less susceptible to irradiation. It is also more resistant to scratches and less hydroscopic than Lithium Fluoride.[7]

Magnesium Fluoride was selected for the sensor window. The thermal expansion coefficient of MgF_2 is considerably different from that of glass. Special techniques were developed to seal the window to the tube. Gold foil is cemented to the MgF_2 window with a frit glass. The gold foil is then electron beam welded to a Kovar fringe which is subsequently welded to a mating Kovar

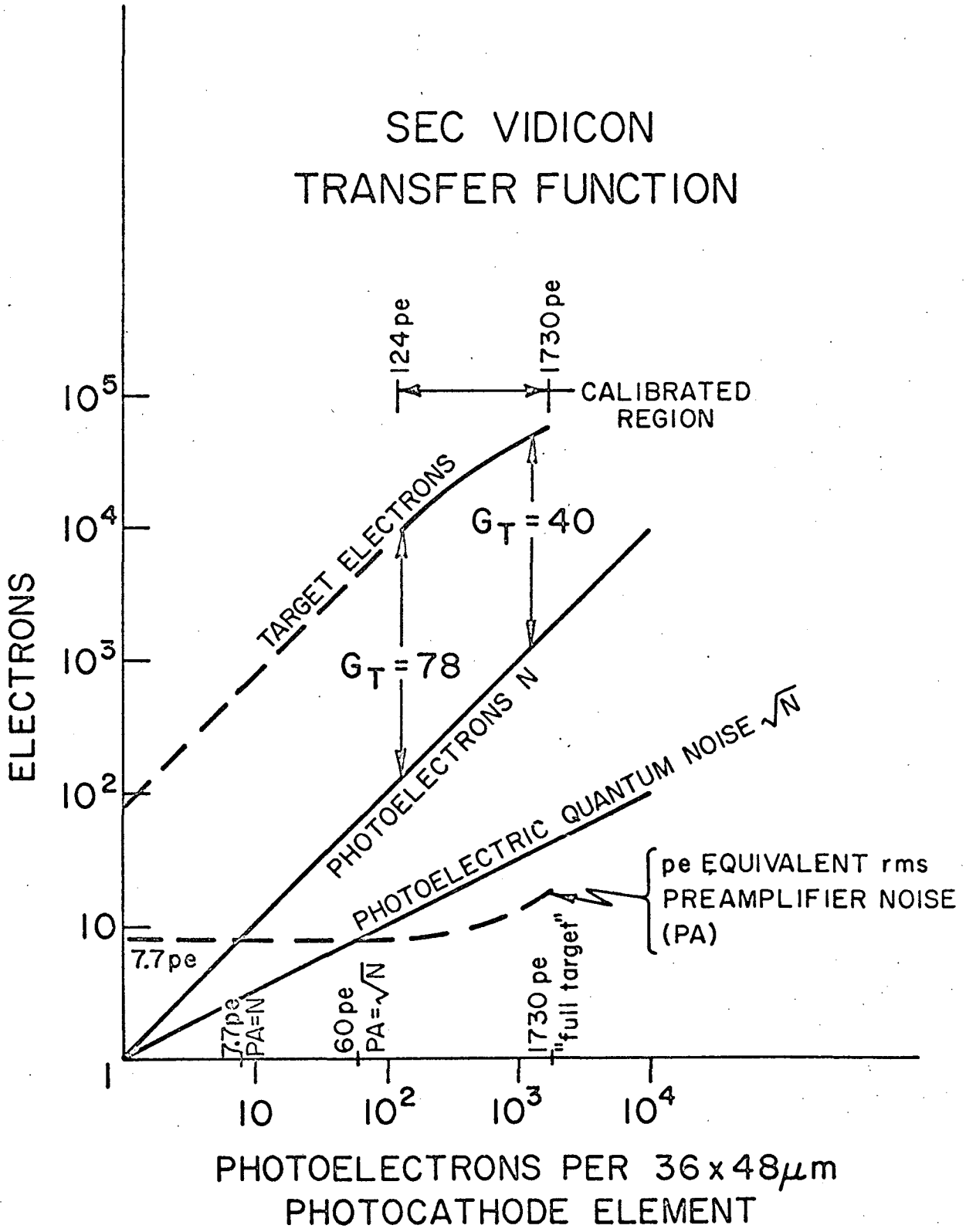

Figure 5 - SEC-Vidicon Photoelectric Transfer Function.

flange. Kovar closely matches the thermal expansion coefficient of glass.

The photocathode is a bi-alkali ($Na_2K\ S_b$) which exhibits high quantum efficiency from 5000A° into the far ultraviolet. The spectral response of the MgF_2 window, bialkali photocathode, combination has been measured in completed tubes and found to be approximately 14% at 1216 and 1608A°. The number of tubes measured is quite small but several tubes are currently being fabricated to demonstrate the ultraviolet capability of the WX-31718.

Red response is sacrificed to reduce the internal background in the tube. Cesium used to improve red sensitivity also results in enhanced dark emission from the photocathode and enhanced field emission from the walls of the image section. For measurements in the red and near infrared the current plan is to fiber optically couple an image intensifier to the sensor which has a special infrared sensitive photocathode. These "III-V" photocathodes are being developed in image intensifiers by the Dept. of Defense and are sensitive out to about 1.1 micron. The prospects are good that this can be extended to 1.6 micron.

With the proposed approach of fiber optically coupling the two devices, it is possible to circumvent the expense of developing a television sensor with this special cathode.

For wavelengths shortward of the MgF_2 cutoff at 1150A°, a similar approach could be used, i.e., fiber optically coupling an image intensifier to the SEC-vidicon. In this case the intensifier would be a windowless cassigrain configuration with the photocathode on the secondary. This configuration has been successfully employed by Carruthers at the United States Naval Research Laboratory using photographic film in place of the the phosphor output.[11]

An alternative is to use channel multiplier plates that are sensitive to high energy photons. The output in this case could be a phosphor coupled via fiber optics to the integrating television tube.

There are no definite plans in this area at Princeton but suitable components could be developed for the LST as the experimental requirements become evident.

Resolution

The resolution of the image sensor, often referred to as its modulation transfer function (MTF), is made up of the product of the MTF of the image section, the target, and the readout section.

Image Section MTF

The magnetically focused image section exhibits very high resolution when the voltage gradient between the photocathode and target is high. The theoretical square wave MTF of the image section in the WX31718 is shown in Figure 6 as a function of the photoelectron energy.[8] There is experimental evidence that it approaches this performance in the actual tube.

The photoelectron energy or velocity is a function of the photon energy, the band gap energy, and electron affinity of the photocathode. The bialkali ($Na_2K\ Sb$) photocathode used in the WX-31718 has an electron affinity of 1.0 volt and a band gap of 1.0 volt. The resultant velocity distribution is shown in Figure 7 for various photon energies.[9] Pair production of electrons in the semiconductor photocathode begins at 3 times the band gap. On the average, one of the two electrons resulting from the high energy photon escapes, but at low velocity. This pair production flattens the quantum yield and limits the high

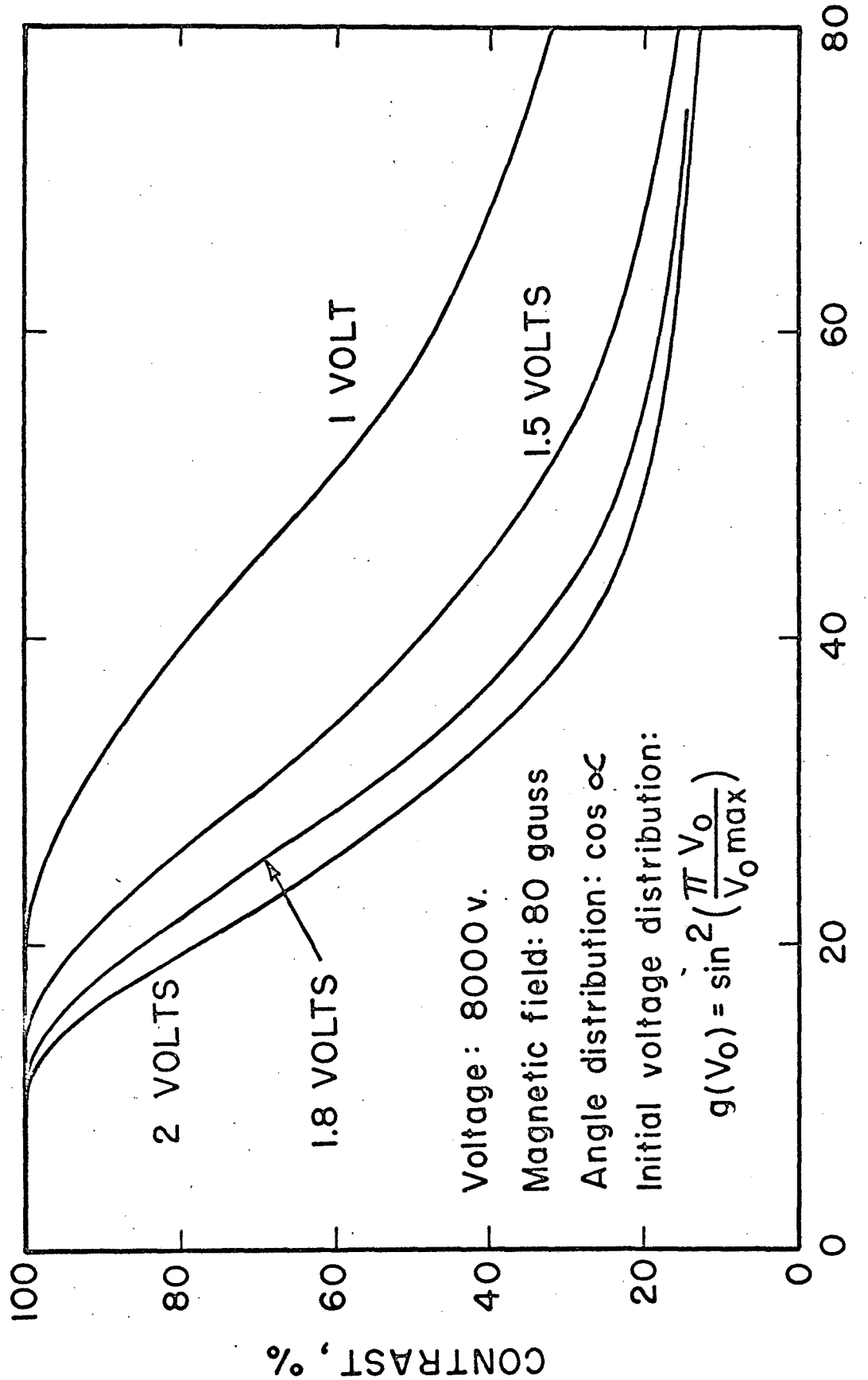

Figure 6 - Magnetic Focused Image Section MTF.

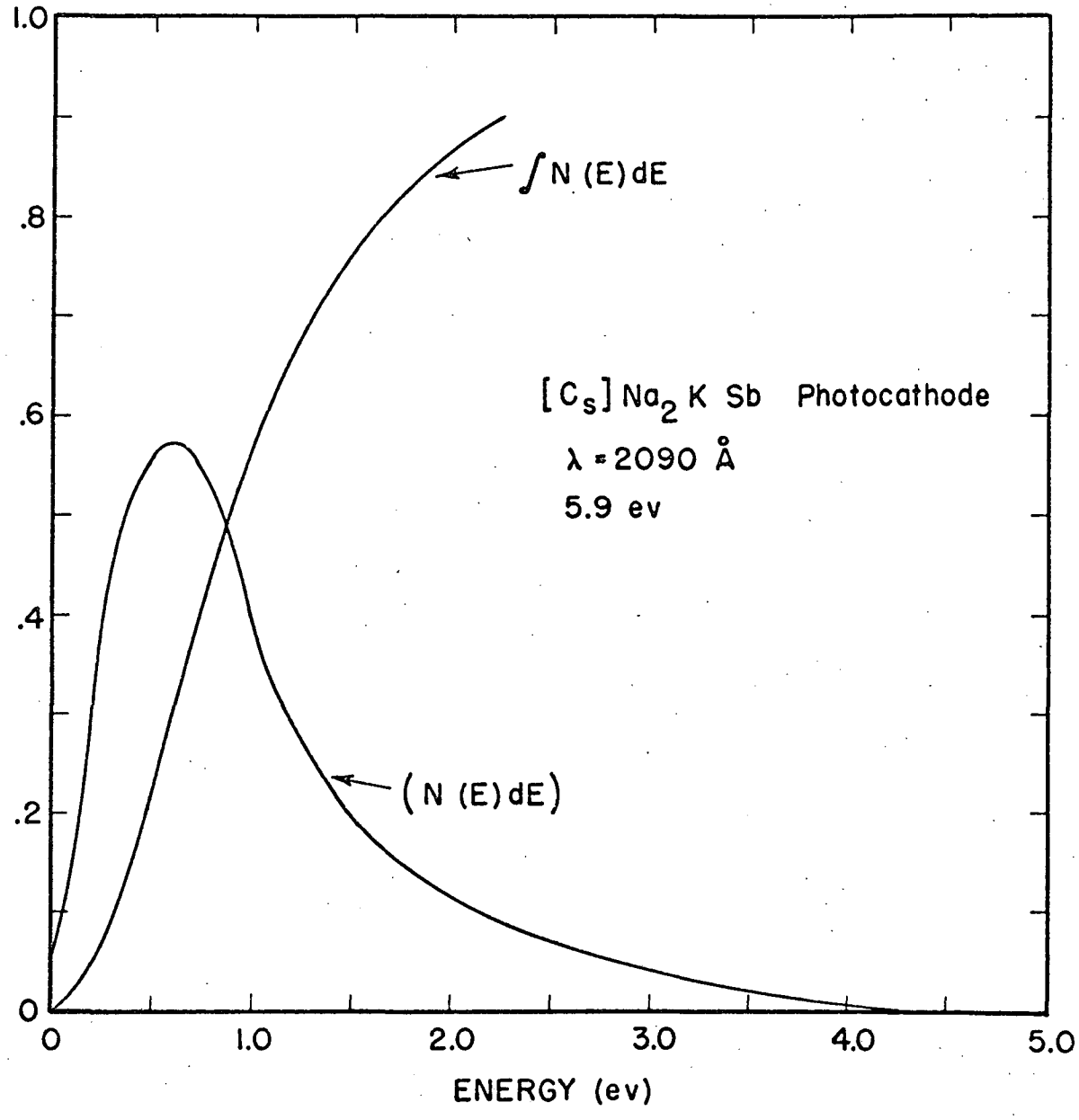

Figure 7 - Photoelectron Velocity Distribution.

energy photoelectrons to a small fraction of the total emitted.[10] The curve for 5.9 ev is representative of higher energy photons as well, with a gradual extension of the high energy tail of the curve as the photon energy increases.

This makes the bialkali photocathode very desirable for ultraviolet applications where low sensitivity at longer wavelengths is not a requirement. One can expect a relative degradation in resolution with solar blind photocathodes such as C_sI due to the higher energy of the emitted photocathodes.

Target MTF

The target MTF is a function of the effective thickness of the dielectric layer separating the readout beam from the signal plate as it recharges the target to cathode potential.[12] This function is plotted in Figure 8 for various thicknesses.

The most recent MTF measurements of the WX-31718 with an improved deflection yoke are also shown in Figure 8 . Measurements of the target capacitance indicate a target thickness of about 7 microns. Therefore one concludes that the effective thickness as related to the MTF calculation is not directly obtained from the capacitance measurement. One may also conclude that the present resolution of the WX-31718 is dominated by the target and can be improved by going to a target that is thinner as seen by the reading beam.

The theoretical resolution of the electron bombarded silicon EBS-vidicon is shown in Figure 9. One notes that the target MTF again dominates the overall MTF and is made up of three factors, the diode sampling, the lateral diffusion, and the electrostatic thickness as discussed above. The net MTF is comparable to the SEC-vidicon. However, silicon targets with 8 micron diode spacing are still in the experimental phase and the actual performance may be less than the prediction in Figure 9.

Readout Section

The resolution of the readout section is primarily the aperture response of the electron beam. The analysis of this response is complicated and may be found elsewhere.[13] In general, the magnetically focused beam has higher resolution than electrostatic focus, the resolution increases at slow scan due to a lower beam current and a correspondingly smaller beam width. There is also a self sharpening effect in the readout process due to the leading edge of the beam doing most of the recharging of the charge depleted areas on the exposed portion of the target. The trailing edge of the beam sees a fully charged target resulting in a reading beam that is effectively more narrow than the actual physical width of the electron beam. The electron beam MTF shown in Figure 9 is representative of the current state of the art.

IV. CURRENT STATUS OF SEC-VIDICON DEVELOPMENT

The development program has concentrated on three important areas, ultraviolet sensitivity, low internal background for long exposures, and ruggedization to withstand the launch environment. It is rewarding to report that success has been achieved in each of these areas as well as other important aspects of the sensor's performance.

After considerable difficulty a reliable technique was found for sealing Magnesium Fluoride windows to the front of the image section. With this "gold foil" technique there has been 100% success. Difficulty was also encountered in obtaining good quantum efficiency photocathodes on Magnesium Fluoride. Recent results indicate that this problem is also solved.

The resolution of the sensor has been substantially improved by a new deflection yoke and the latest results are shown in Figure 8. This resolution

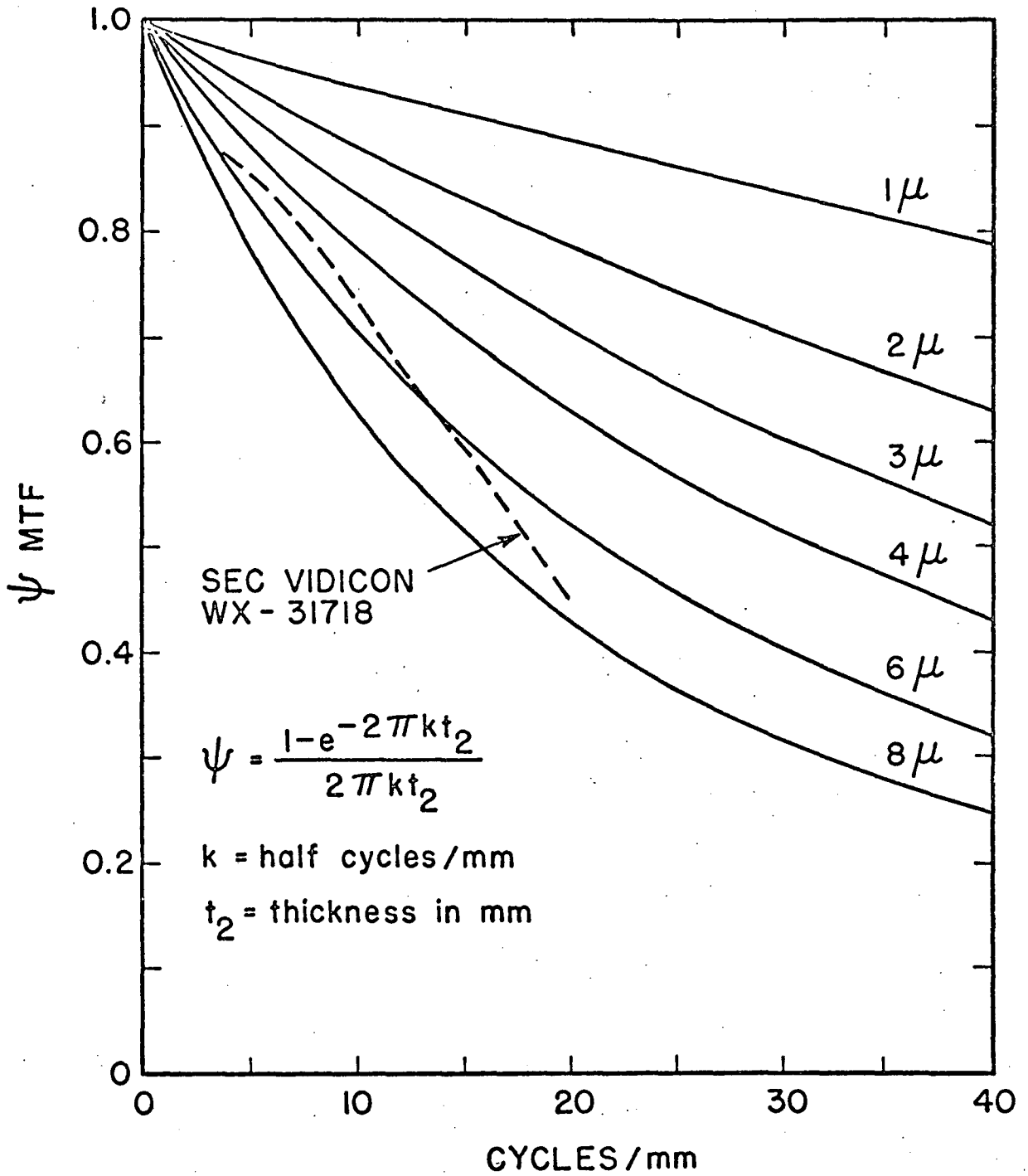

Figure 8 - Target MTF vs. Target Thickness.

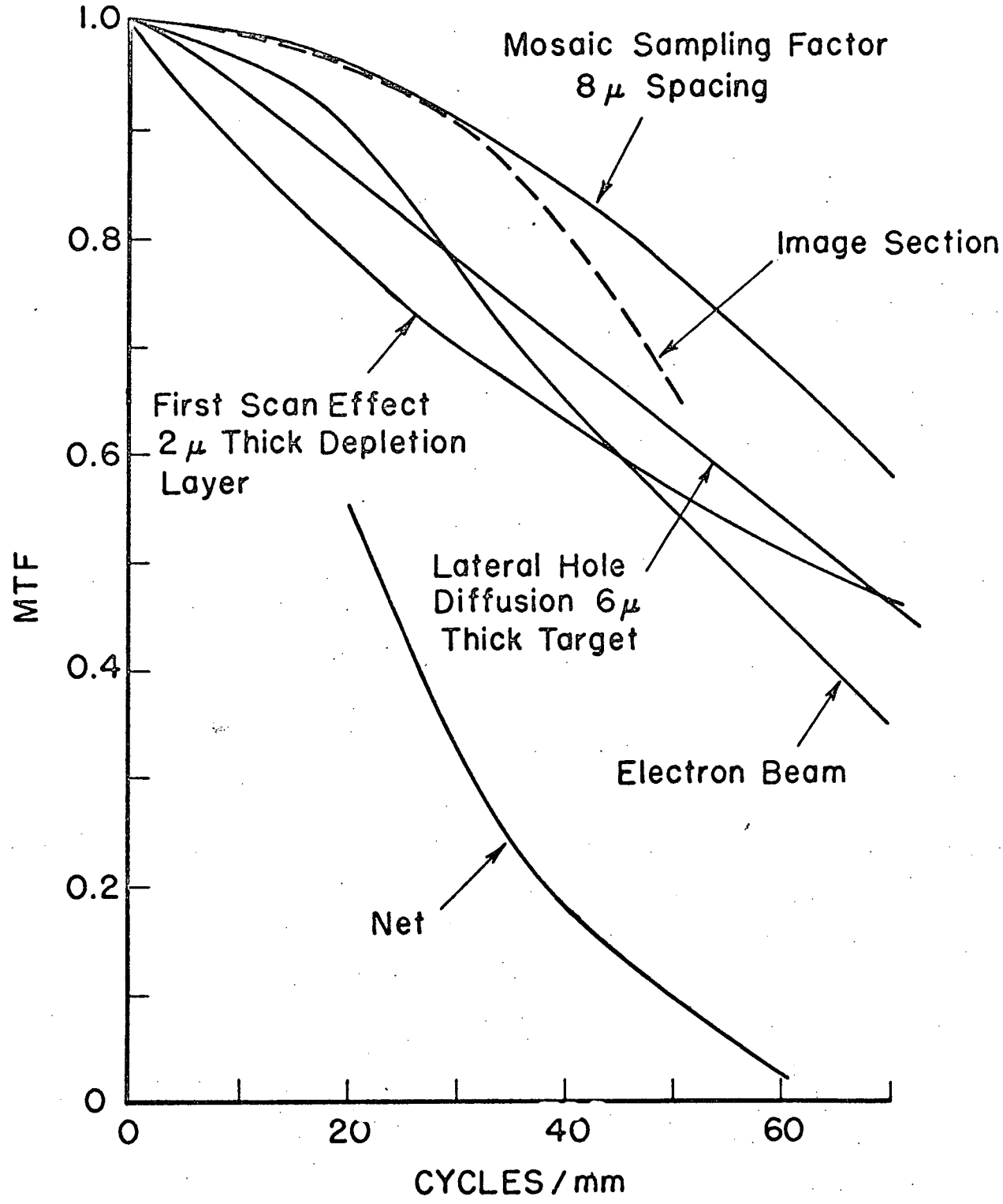

Figure 9 - Theoretical MTF of EBS-Vidicon.

appears to be dominated by the target MTF and it is anticipated that a new high capacity target now under development will exhibit higher resolution.

The photoelectric transfer function is shown in Figure 5, and one notes that the signal to noise ratio is dominated by the statistical noise in the photoelectrons over a substantial portion of the dynamic range. The readout noise is less than 8 photoelectron rms per picture element.

The ruggedization results, while statistically meager, do indicate that the 25 mm x 25 mm target and the gold foil window seal are sturdy enough to survive an OAO type launch. The environmental testing is summarized in Table III. Most of the eight tubes currently being built will be used for further environmental testing and then put on life test to evaluate the life of the electron gun when operated in the proposed low current, on-off mode anticipated in the LST mission.

TABLE III

Summary Of Environmental Testing Of WX-31718 SEC-Vidicon

Thermal Shock +25°C to -55°C

Two tubes tested
Result-No degradation

Shock 15g & 30g

One tube tested
Result-No degradation

Shock, No Vacuum 15g

One tube tested
Result-No degradation

Acceleration 35g for 4 minutes

Two tubes tested
Result-No degradation

Vibration 10 to 2000 Hz

Results: No problem with MgF_2 window for 14g to 110 Hz, and 7.5g from 110 to 2000 Hz.

One tube also vibrated without vacuum.

Spots develop in target when vibrated above 5g in region from 110 to 2000 Hz.

V. PLANS

Further Improvements to WX-31718 SEC-Vidicon

The next phase in the image sensor development will be to incorporate a higher capacitance target in the WX-31718. This is expected to increase the dynamic range and also improve the target MTF since the higher capacitance target should exhibit a lower effective thickness. Work will also be initiated to make a red sensitive version of the tube and still maintain the low internal

background in the image section in the presence of Cesium. In many respects the 25 mm tube will continue to serve as the precursor for the large tube development discussed below.

Near Infrared Image Sensors

As noted in the section, Spectral Sensitivity, image intensifiers are being developed by the Department of Defense that exhibit very high quantum efficiency out to about 1.1 micron. The plan is to fiber optically couple these III-V photocathode intensifiers to the existing WX-31718 SEC-vidicon or an EBS-vidicon. This will, hopefully, maintain the long integration capability and double the overall spectral coverage possible with these quantum noise limited image sensors. It is anticipated that the internal background of the sensor system will be increased due to the Cesium in the image intensifier that is necessary to achieve the red sensitivity.

Large Tube Development

As discussed earlier, the high angular resolution of the LST will result in 14,500 picture elements across the 4 arc minute field of view. The 25 mm wide format and the MTF of the current SEC-vidicon limits the field to 1000 picture elements which corresponds to 17 seconds of arc. This is considered marginal and a program has recently been initiated to improve the total resolution of the image sensor, both by increasing the MTF in cycles per mm and also by enlarging the image area.

The first step will be to determine the feasibility of making a higher capacity SEC target that is 50 mm x 50 mm and rugged enough to withstand the launch environment. Target substrates of aluminum oxide will be fabricated and mounted on a 50 mm x 50 mm frame. This subassembly will be mounted in a vacuum tight enclosure and subjected to environmental tests. Targets with a narrow support down the middle will also be considered. An attractive alternative to the large diaphram is a solid substrate target. In this case the target must be exposed and read out from the same side. Rotating the target 180° for read and write appears to be the best scheme and does appear feasible with proven techniques. With a solid substrate the target size is no longer limited by fragility, but by the electron optics required to achieve a uniform high resolution scan of the larger area by the electron reading beam.

A higher capacitance target is highly desirable to maintain the dynamic range in photoelectrons per picture element as the picture elements are made physically smaller. It also appears necessary to make the KCl layer thinner in order to improve the intrinsic resolution of the target in first scan readout, (see Figure 8). Fortunately higher capacitance targets can also be expected to be thinner.

The possibility of a large silicon target tube is also being explored. The main uncertainty here is, again, the manufacturability and ruggedness of the thin silicon diaphram. Equally important is the question of target dark current, i.e., the period over which it can integrate.

It may be possible to develop a basic large tube that could take either the SEC or silicon diode target. The silicon targets are made by several manufacturers including RCA and Texas Instruments.

Pre-LST Applications

The importance of the LST mission makes it equally important that the image sensors perform well and reliably. An important part of the image sensor development has been to use the SEC-vidicon for actual scientific observations.

The 25 mm format tube has been used by Princeton in collaboration with Cal Tech astronomers on the 60-inch reflector at Mt. Wilson and on the 200-inch Hale Telescope at Palomar Mountain. The television system has also been used at Princeton and Kitt Peak. Figure 10 shows the spectrum of the Quasar PHL 957 obtained on the Coudé Spectrograph of the 200-inch telescope in a six hour exposure. The spectral resolution is 0.75A° and the exposure was about 785 photoelectrons per Ångstrom.

A television camera is currently being built for Flight 9 of Stratoscope II, expected to occur in early 1973. This camera will replace the 70 mm film camera and is expected to increase the system sensitivity by at least two stellar magnitudes. This flight will also be a very good test of the television sensor's performance with a nearly diffraction limited telescope.

A second television camera is being built for a sounding rocket payload. As shown in Figure 11 the television camera records the spectra from an objective grating echelle spectrograph covering the spectral region from 1150A° to 1800A° with a $\frac{\lambda}{\Delta\lambda}$ of 10^4. This payload will be launched during the summer of 1972.

VI. GROUND BASED OBSERVATIONAL RESULTS

The work to date has greatly benefited from use of the sensor in ground based observations at Princeton and other observatories. A better insight into the data reduction problems has led to sensor improvements and the development of computer programs that will be useful in later space applications. The observational programs to date are briefly discussed below.

A. High Dispersion Spectroscopy on 200-inch Coudé Spectrograph

The most notable achievement to date has been the observations of very faint quasi-stellar objects and galaxies at high dispersion on the 200-inch Hale telescope's Coudé spectrograph. Spectra of the radio quiet quasar PHL 957 (V-16.5 mag) were obtained from 4270 to 4495° with 0.75A° resolution in a 6 hour exposure. Thirty one absorption lines were recorded and several of the lines were resolved and reach zero central intensity. Figure 10 shows the unwidened Coudé spectrum of PHL 957 obtained on October 9, 1970 in a 6 hour exposure with the integrating television camera using the SEC-vidicon, WX-31718. The horizontal lines are the television scan lines which the smallest rectangles on each line are the digital picture elements whose widths corresponds to one third the net resolution of 0.75A°. The vertical scale has been magnified 4.5 times relative to the horizontal scale. The comparison spectrum is an iron arc and the emission line crossing the spectrum left of center is the 4358.3A° line of HgI in the night sky. The intensity trace of the same spectrum is also shown in Figure 12.

B. High Dispersion Spectroscopy on Princeton 36-inch and Mt. Wilson 60-inch

The television system has been used with a half meter Ebert-Faste spectrograph for high dispersion spectrographic observations. The output is magnified by 2.25 :1 resulting in a dispersion of 3.5A°/mm at the photocathode. Figure 12 shows the spectrum of two stars, Lambda Hya (M_v = 3.62) and Gamma Tau (M_v = 3.66) taken in 15 minute exposures on the Princeton 36" reflector during the winter.

C. Photometry of Galaxies

The television system has been used at Princeton and Kitt Peak by P. Crane of Princeton to do photometry of galaxies. Figure 13 shows an image of the galaxy NGC 3842 obtained on the Kitt Peak 36" reflector. An advantage of the television system for this work is the fact that the data is recorded on magnetic tape and can therefore be easily analyzed by computer as shown by the equal brightness contours in Figure 14 of the double galaxy NGC 3845.

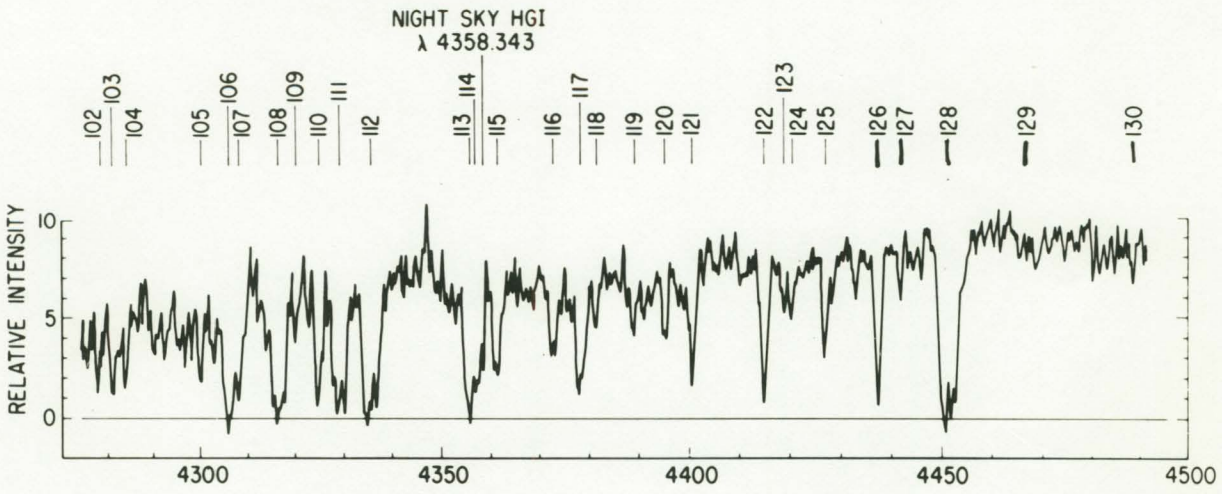

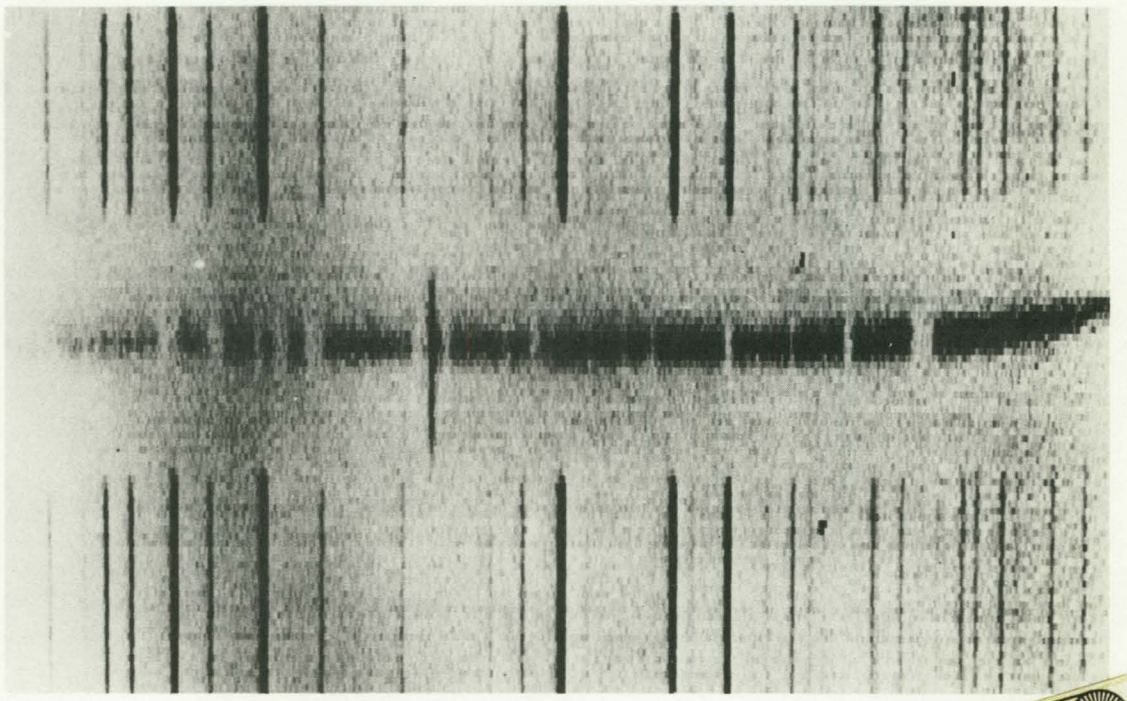

Figure 10

Spectrum of the Quasar PHL-957, obtained with Princeton Integrating TV System on Hale 200" Coude Spectrograph.

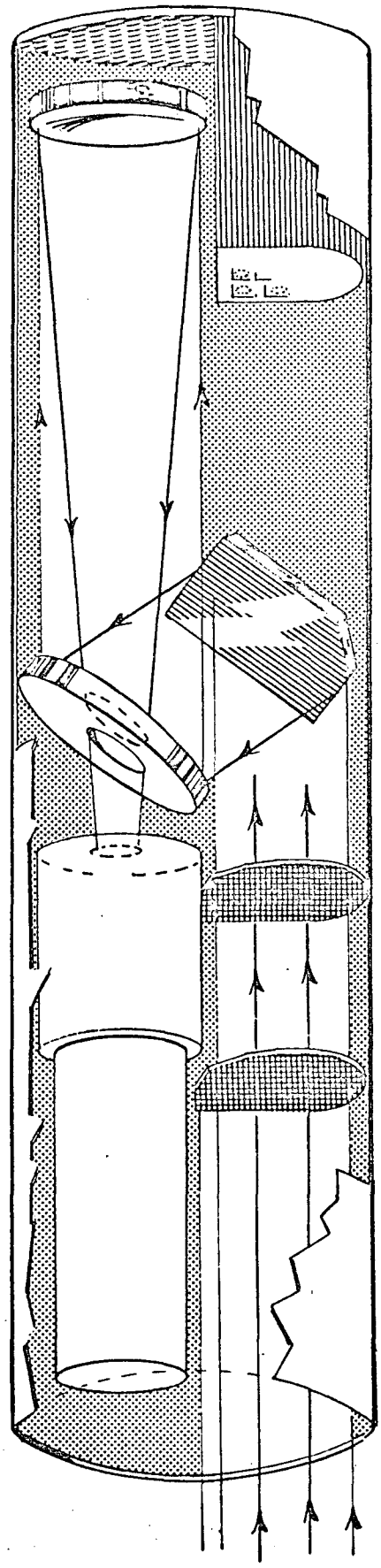

Figure 11 - UV Echelle Spectrograph-TV Payload for Sounding Rocket.

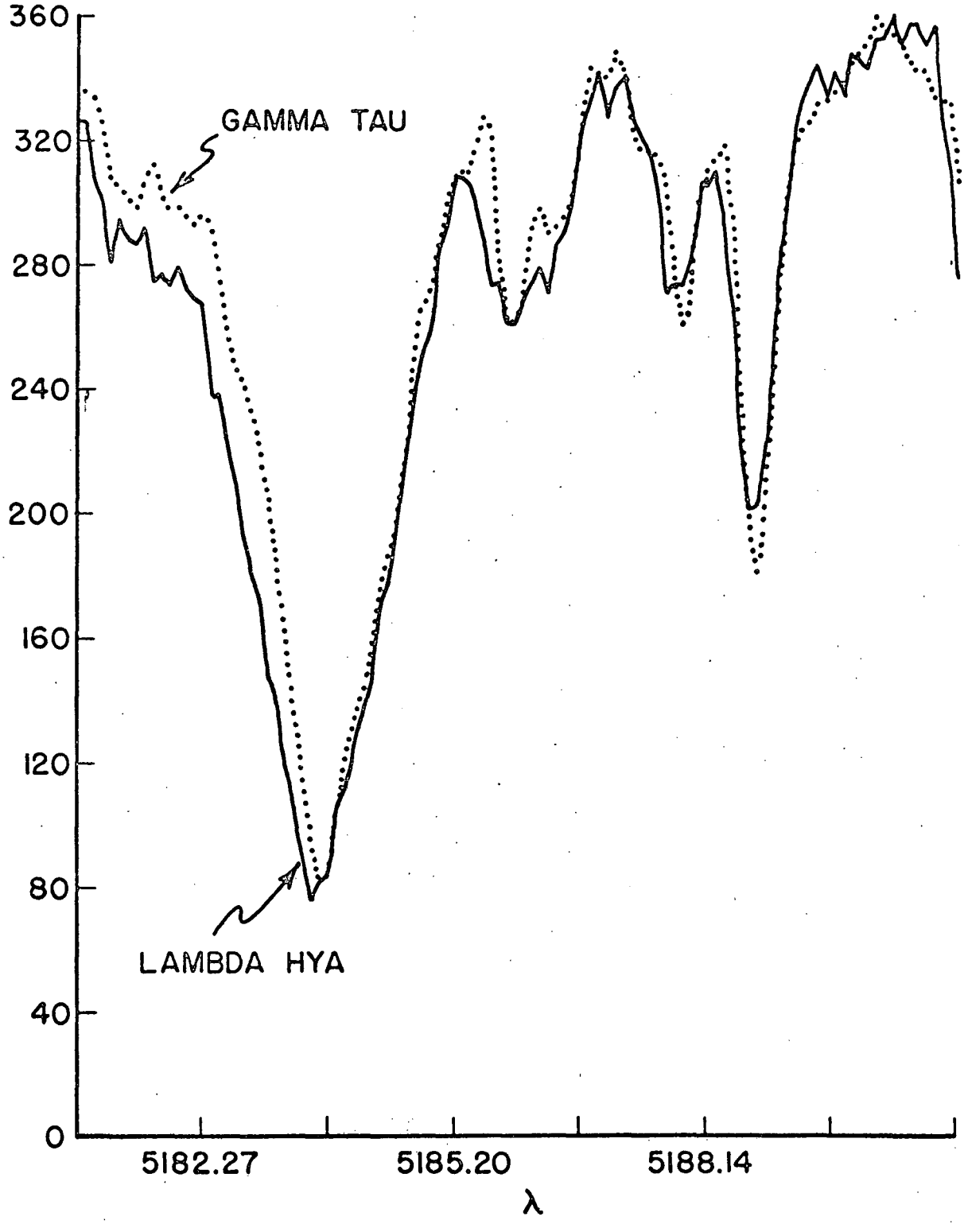

Figure 12 - Spectra of Lambda Hya and Gamma Tau, 15 minute exposures on 36" Princeton Telescope with TV System.

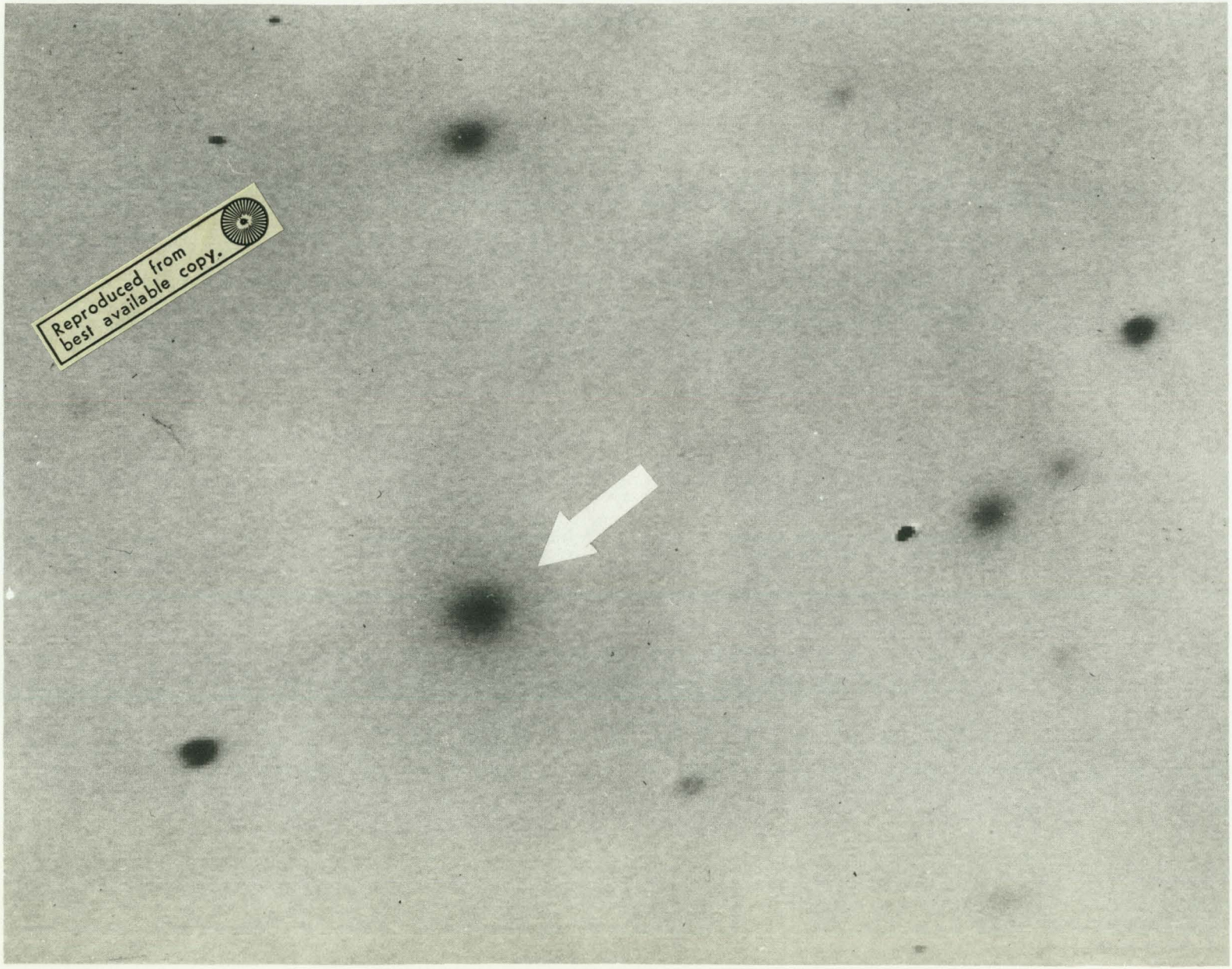

Figure 13 - Galaxy NGC 3842 taken with Princeton Integrating TV on Kitt Peak 36" telescope, 2.5 minute exposure at f/13.5.

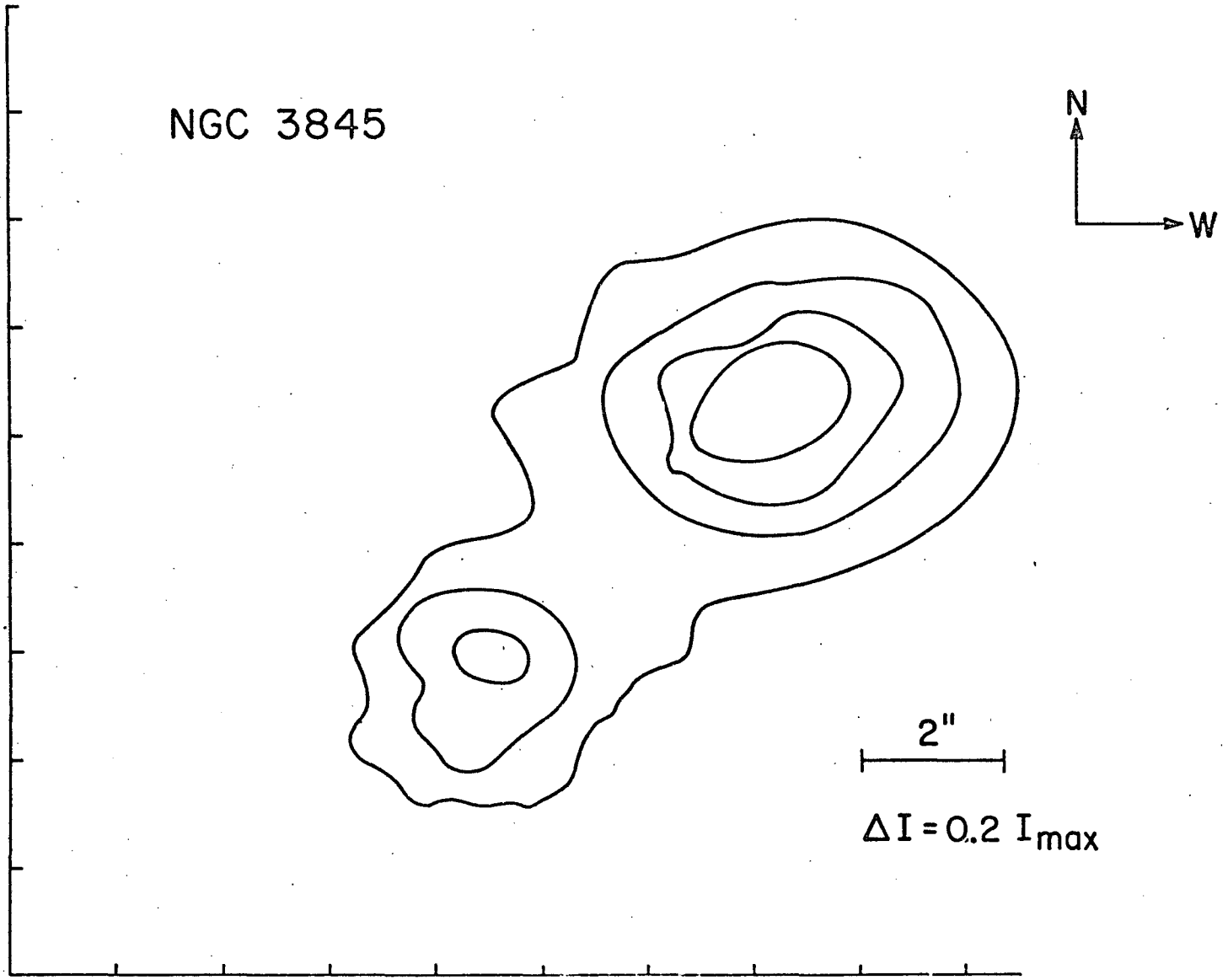

Figure 14 - Equal Brightness Contours of NGC 3845.

VII. ACKNOWLEDGEMENTS

This work is supported by NASA Headquarters under NSR-31-001-127 and NGR-31-001-236. The authors are indebted to Dr. R. Bohlin, University of Colorado, and E. Wilson, Princeton Observatory for ultraviolet sensitivity measurements, to Dr. D. Morton, Dr. B. Taylor and Dr. P. Crane for the examples of astronomical observations with the television system, and to J. Opperman and P. Murray for making many of the laboratory measurements.

REFERENCES

1. Zucchino, P., and Lowrance, J. L., "Progress Report on Development of the SEC-Vidicon for Astronomy", Astronomical Use of Television Type Sensors, Symposium Proceedings, Princeton Observatory, May 20-21, 1970, NASA SP-256, pp. 27-53 (1971).

2. Lowrance, J. L., and Zucchino, P., Advances in Electronics and Electron Physics, Vol. 28B, pp. 851-874, Academic Press, London (1969).

3. Beurle, R. L., Proc. Institute Elect. Engr., 110, p. 1350 (1963).

4. Schwartz, M., Information Transmission, Modulation and Noise, pp. 151-154, McGraw-Hill, New York (1970).

5. Black, H. S., Modulation Theory, Chapt. 4, Van Nostrand, Princeton, N. J. (1953).

6. Rome, M., Photoelectric Imaging Devices, Vol. 1, Plenum Press, New York (1971).

7. Heath, D. F., and Sacher, P. A., Applied Optics, Vol. 5, No. 6, pp. 937-943, (1966).

8. Pietrzyk, J. P., Westinghouse Corporation, private communication (1971).

9. Spicer, W. E., J. Phys. Chem. Solids, Vol. 22, pp. 365-370, Pergamon Press, New York (1961).

10. Spicer, W. E., private communication (1971).

11. Carruthers, G. R., Applied Optics, Vol. 8, pp. 633-638 (1969).

12. Krittman, I. M., "Resolution of Electrostatic Storage Targets", IEEE Transactions on Electronic Devices, Vol. 10, November 1963.

13. Shade, O. H., RCA Review, Vol. 31, No. 1, pp. 60-119, March 1970.